The Journal of Antibiotics (2009) 62, 519–526

www.nature.com/ja

ORIGINAL ARTICLE

Salinisporamycin, a novel metabolite from *Salinispora arenicora*

Satoru Matsuda[1], Kyoko Adachi[1], Yoshihide Matsuo[1], Manabu Nukina[2] and Yoshikazu Shizuri[3]

A new rifamycin antibiotic, salinisporamycin (1), has been isolated from a culture of a marine actinomycete. The producing organism was identified as *Salinispora arenicora* on the basis of the 16S rRNA sequence. High-resolution FAB-MS established the molecular formula of 1 as $C_{33}H_{43}NO_9$. The planar structure of 1 was elucidated by NMR spectral analysis including COSY, heteronuclear single quantum coherence and heteronuclear multiple bond correlation. The relative stereochemistry of 1 was determined on the basis of rotating frame nuclear Overhauser effect spectroscopy. In addition, the solvatochromic behavior of 1 was investigated by measuring the UV spectra. This compound inhibited the growth of A549 cells, the human lung adenocarcinoma cell line, with an IC_{50} value of 3 μg ml^{-1}, and also showed antimicrobial activity.
The Journal of Antibiotics (2009) **62,** 519–526; doi:10.1038/ja.2009.75; published online 7 August 2009

Keywords: antimicrobial; cytotoxic; rifamycin antibiotic; salinisporamycin; *Salinispora arenicora*; YM23-082

INTRODUCTION

It is thought that the exploration of novel natural products in the marine environment is valuable in view of the diversity of marine microbial and metabolic products.[1] Novel marine natural products have been reported on a continuous basis.[2] Therefore, it can be expected that the LC-MS (HPLC/PDA-ESI-MS) system with simulated data of many antibiotics and others may have an important role for identification of many classes of novel marine natural products.[3,4]

Salinispora sp. was identified as the first seawater-requiring marine actinomycete.[1,5] This bacterium includes the potent proteasome inhibitor salinosporamide A, which is under investigation in a phase 1 clinical trial for the treatment of cancer.[1,6,7] The analysis of the *Salinispora tropica* genome revealed the presence of a polyketide synthase system and nonribosomal peptide synthases, with a large percentage of its genome (~10%) devoted to secondary metabolite biosynthesis, which is greater than the *Streptomyces* genome sequence.[1,7]

In this study, we investigated bioactive products from *Salinispora* sp. Results of this screening showed that YM23-082 extracts had strong antitumor and antimicrobial activities among 17 species of *Salinispora*. Therefore, bioactive products were isolated from YM23-082 extracts using LC-MS methods. The results showed hat saliniketals A (**2**)[8,9] and rifamycin S (**3**)[10] were isolated from YM23-082 extracts. In salinisporamycin (**1**), it was expected that the ansa chain partial structure could be assigned as saliniketals[8,9] and connected to the naphthoquinone ring system. **1** and **2** show structural resemblance to the construct of rifamycin antibiotics. Therefore, **1** and **2** would be biosynthetically related products of rifamycin antibiotics. Also, **1** showed moderate cytotoxic activity against A549 and antimicrobial activities. Their structures are shown in Figure 1.

In our study, we elucidated the taxonomy, physicochemical properties, structure and biological activity of salinisporamycin (**1**) from *Salinispora arenicora* YM23-082.

RESULTS AND DISCUSSION

Identification of taxonomy

The strain YM23-082 was isolated from marine sediment collected in the Yap State in the Federated States of Micronesia, N: 9°31′11.0″, E: 138°10′26.7″ and grew at room temperature on a marine agar 2206 (BD Difco, Tokyo, Japan) plate. The culture YM23-082 showed colonies and an orange pigment was produced frequently.[5] The 16S rRNA sequencing of this strain revealed high sequence identity with *S. arenicola* CNH643 (AY040619.2) (100.0%).[5] This strain included **2**, **3**, staurosporine and K-252C[6] (data not shown). On account of this characteristic, the strain YM23-082 was tentatively identified as a member of the *S. arenicora* CNH643.

Physicochemical properties

The physicochemical properties of **1** are summarized in Table 1. **1** was isolated as an amorphous compound ($[\alpha]_D^{24}$ +36.0, *c* 0.7, MeOH). It was soluble in DMSO, MeOH, Me_2CO and $CHCl_3$, poorly soluble in water, and insoluble in n-Hex. **1** was identified as having an R_F value at 0.84 ($CHCl_3$:MeOH=4:1). Analysis of LC-MS spectral data on positive and negative ions revealed the molecular mass to be 597. The molecular formula of **1** was established as $C_{33}H_{43}NO_9$

[1]Bioorganic Chemistry Group, Marine Biotechnology Institute Co. Ltd., Kamaishi, Iwate, Japan; [2]The United Graduate School of Agricultural Sciences, Iwate University (Yamagata University), Tsuruoka, Yamagata, Japan and [3]MBI chair 'Marine Biosciences', Kamaishi Research Laboratory, Kitasato University, Kamaishi, Iwate, Japan
Correspondence: S Matsuda, Bioorganic Chemistry Group, Marine Biotechnology Institute Co. Ltd. 3-75-1 Heita, Kamaishi, Iwate 026-0001, Japan.
E-mail: s-matsuda@amail.plala.or.jp
Received 17 May 2009; revised 9 July 2009; accepted 13 July 2009; published online 7 August 2009

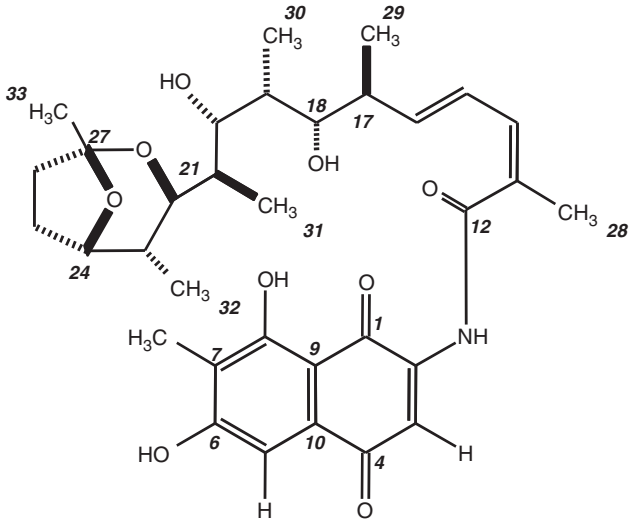

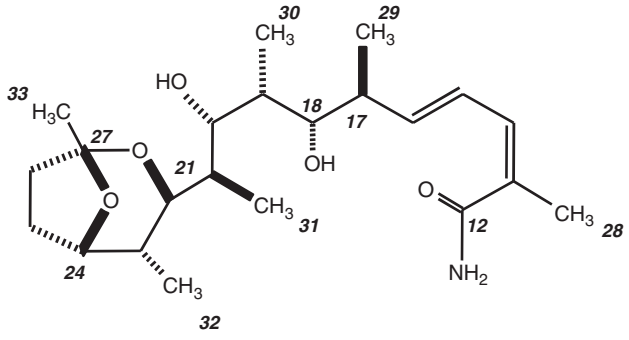

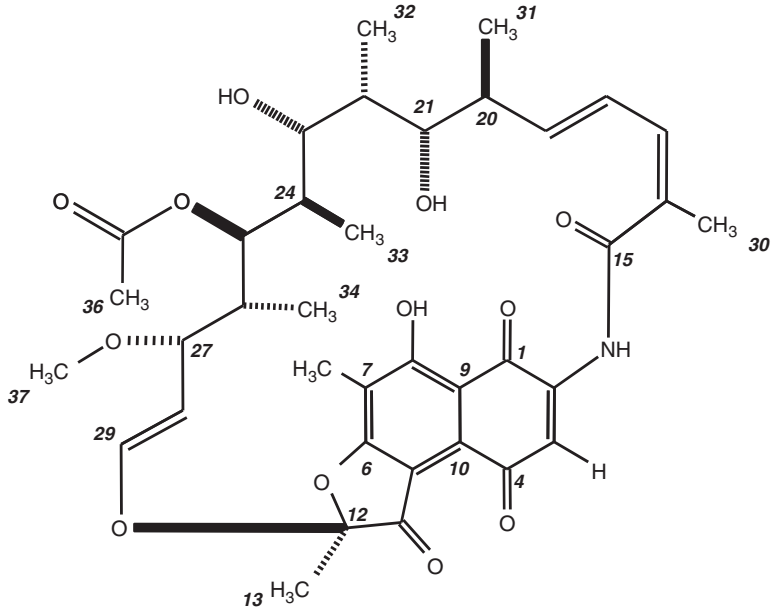

Figure 1 Structures of salinisporamycin (**1**), saliniketal A (**2**) and rifamycin S (**3**).

by high-resolution FAB-MS data ($[M+H]^+$: found, *m/z* 598.3027, calcd for $C_{33}H_{44}NO_9$, *m/z* 598.3011). In addition, the exchangeable protons of **1** were established by hydrogen–deuterium (H–D) exchange mass spectrometry (ESI-IT-MS, profile mode). The H–D exchange signals were found at *m/z* 625.47 $[M+Na]^+$ (calcd for $C_{33}H_{38}D_5NNaO_9$, *m/z* 625.32) with a dimer ion at *m/z* 1227.13 $[2M+Na]^+$, indicating the presence of the intermolecular exchange of 5 hydrogen atoms (data not shown). The UV spectrum of **1** was nearly identical with that of **3** in solvent MeOH. Also, the UV spectrum of **1** showed a short wavelength at 595 nm in the solvent DMSO. The absorption at 595 nm was possibly due to the presence of conjugated double bonds between the naphthoquinone chromophore and the α-, β-, γ- and δ-unsaturated system. However, the imide-amide tautomeric form of **1** could not be distinguished from the NMR spectral data.

Structural elucidation

^1H and ^{13}C NMR spectral data for **1** are summarized in Table 2. All one-bond ^1H-^{13}C connections were confirmed by heteronuclear single quantum coherence (HSQC) correlations. Two methylene signals at δ_c 24.1 (C-25) and 35.4 (C-26) were observed in the DEPT spectrum and HSQC correlations. Also, other carbon signal types were assigned by the DEPT spectrum and HSQC correlations.

The ansa chain partial structure of **1** was confirmed by COSY and heteronuclear multiple bond correlations (HMBCs) in solvent CD_3OD. These results showed a structural resemblance to the ansa chain of rifamycin antibiotics.[10] These assignments are summarized in Figure 2.

The α-, β-, γ- and δ-unsaturated system signals at δ_H 6.46 (1H, br d, 11.3, H-14), 6.79 (1H, dd, 15.0, 10.9, H-15), 6.03 (1H, dd, 15.0, 8.3, H-16), 2.07 (3H, d, 1.1, CH_3-28) and a quaternary sp^2 carbon

Table 1 Physicochemical properties of 1

Appearance	Amorphous
Molecular formula	$C_{33}H_{43}NO_9$
LC-ESI-MS (*m/z*)	598 $[M+H]^+$
	596 $[M-H]^-$
High-resolution FAB-MS (m/z)	
Found	598.3027 $[M+H]^+$
Calcd	598.3011 $[M+H]^+$
$[\alpha]_D$	+36.0 (*c* 0.7, MeOH)
TLC (R_F value)	$CHCl_3$:MeOH (4:1)
(SiO_2, Merck F_{254})	R_F 0.84
UV λ_{max} nm (log ε) in MeOH	225 (4.66), 272 (4.52), 319 (4.26), 408 (3.83)
UV λ_{max} nm (log ε) in DMSO	281 (4.58), 307 (4.49), 320 (4.49), 358 (4.27), 432 (3.73), 595 (3.69)
IR ν_{max} (KBr) cm^{-1}	3399, 2926, 1600, 1496, 1458, 1387, 1327, 1098, 974

signal at δ_C 129.7 (C-13) were mainly confirmed by $^3J_{HH}$ coupling constants of olefinic protons and HMBC correlations. The $^4J_{HH}$ coupling constant of proton signals at CH_3-28 and H-14 was determined by COSY correlation. In addition, the configuration of C-15/C-16 was assigned as *E* on the basis of the $^3J_{HH}$ coupling constant of H-15/H-16 at 15.0 Hz. This result was supported by the fact that H-14 and CH_3-28 were determined by rotating frame nuclear Overhauser effect spectroscopy (ROESY) correlations (data not shown). Also, the amide bond signals at δ_H 9.14 (1H, br s, 2-NH) and δ_C 167.1 (C-12) were determined by HMBC correlations in solvent DMSO-d_6 (Table 2). This result was supported by assignment of the amide bond as a primary amide on the basis of the molecular formula.

In contrast, for determination of the terminal ansa chain partial structure of **1**, the tetrahydrofuran ring signals at δ_H 4.20 (1H, br dd, 6.8, 3.8, H-24) and the ketal functional group at δ_C 106.6 (C-27) were confirmed by HMBC correlations. Those results were supported by the finding that the IR spectrum showed characteristic absorption bands at 1098 cm^{-1}, indicating the presence of ether bonds in the molecule.

The two exchangeable proton signals at δ_H 4.57 (1H, m, 18-OH) and 4.64 (1H, m, 20-OH) were mainly determined by COSY correlations in solvent DMSO-d_6. In support of these results, exchangeable proton signals were observed in the pre-saturation spectrum in solvent DMSO-d_6, decreasing the integral intensity of the peak area. Also, the IR spectrum showed characteristic absorption bands at 3399 cm^{-1} (3431 cm^{-1} of **3**), indicating the presence of a hydroxyl group in the molecule. Consequently, these results showed a structural resemblance to the saliniketals.[8,9]

In the detailed analysis, the chemical shifts in the ansa chain of **1** were compared with values in the literature reported for saliniketal A[8] (Table 2). The chemical shifts revealed that **1** was nearly identical with the spectra of saliniketal A. In addition, the chiral centers of C-17/C-18, C-18/C-19, C-19/C-20, C-20/C-21, C-21/C-22 and C-22/C-23 were mainly determined by the $^3J_{HH}$ coupling constants, COSY and ROESY correlations (Figure 3, Table 2). These results revealed that $^3J_{HH}$ coupling constants of **1** were almost identical with the literature values reported for saliniketal A[8] and the recorded NMR spectra of **2**. The COSY correlation in the ansa chain partial structure signals at δ_H 3.62 (1H, m, 7.5, H-18) and 1.71 (1H, m, H-19) were not observed in solvent DMSO-d_6, because the torsion angle between H-18/H-19 is close to 90°[11] (Figure 3).

The bicyclic ring structure signals at δ_H 1.93 (1H, m, H-25a), 2.02 (1H, m, H-26a) and 3.94 (1H, br d, 10.5, 1.5, H-22) were determined by ROESY correlations (Figure 4). This result was supported by stereochemical assignments in a bicyclic ring structure that a diaxial arrangement signals at δ_H 3.82 (1H, br d, 10.5, 0.9, H-22) and 1.84 (1H, br dq, 10.5, 6.8, 3.8, H-23), and was confirmed by a large coupling constant at 10.5 Hz (Figures 3 and 4). Consequently, the ansa chain of **1** was established to be the same as saliniketal.[8,9]

The naphthoquinone ring system of **1** was mainly confirmed by the ^{13}C NMR spectral data and HMBC correlations (Figure 2, Table 3). With the help of a detailed analysis, the quaternary carbon signal at δ_C 164.5 (C-6) and other carbon signals were nearly identical with values reported in the literature for 31-homorifamycin W.[12] The two quaternary carbon signals at δ_c 181.3 (br, C-1) and 172.0 (br, C-8) gave broad peak signals possibly due to tautomerization (Table 3). These results were supported by the finding that the IR and UV spectra showed characteristic absorption bands at 1496 cm^{-1} (1465 cm^{-1} of **3**) and wavelengths at 319 and 408 nm (315 and 410 nm of **3**), indicating the presence of a chromophoric system in the naphthoquinone form.[10,12] In addition, the IR spectrum showed a characteristic absorption band at 1600 cm^{-1} (1606 cm^{-1} of **3**), indicating the presence of a naphthoquinone carbonyl group linked in the intramolecular hydrogen bond.[12]

The naphthoquinone ring system of **1** was established by the ^{13}C NMR spectral data and HMBC correlations in solvent DMSO-d_6 (Table 3, Figure 5). With the help of a detailed analysis, the naphthoquinone ring system of **1** had chemical shifts comparable to the literature values reported for rifamycin Z.[13] This result revealed that the ^{13}C NMR signals at δ_C 170.3 (C-1, diff. (−11.5 p.p.m.)) and δ_C 180.4 (br, C-6, diff. (+20.4 p.p.m.)) could not be distinguished from the spectra of rifamycin Z. Therefore, the quaternary carbon signal at C-6 was assigned as a carbonyl carbon on the basis of its chemical shift. Intriguingly, the two quaternary carbon signals at δ_c 180.4 (br, C-6) and 162.1 (br, C-8) gave broad peak signals possibly due to tautomerization. The enolic proton signal at δ_H 12.55 (1H, br s, 8-OH) was confirmed by HMBC correlations in solvent DMSO-d_6. These results were supported from the assignment of ^1H-^{13}C connections made by HSQC correlations in solvent DMSO-d_6. Consequently, these results showed the isomerization of the naphthoquinone ring system of **1** by different solvents. However, the enolic proton signal (1-OH) was not determined by the ^1H NMR spectral data (Table 3). Finally, the amide bond between the ansa chain and the naphthoquinone ring system signals at δ_H 9.14 (1H, br s, 2-NH) and δ_C 111.7 (C-3) were determined by HMBC correlations in solvent DMSO-d_6. These results were supported by the finding by H–D exchange mass spectrometry that showed the characteristic intermolecular exchange of five hydrogen atoms.

Biological activity

Compound **1** showed moderate cytotoxic activity against A549 cells with an IC_{50} value of 3 μg ml^{-1}. Compound **3** did not show cytotoxic activity against A549 cells at 200 μg ml^{-1}.[10,12,14] Among all rifamycin antibiotics, **1** showed cytotoxic activity.[14]

The antimicrobial activity of **1** was tested against six microorganisms by paper disk methods. This compound showed moderate activity against two microorganisms (Table 4). The antimicrobial activity of **1** was shown to be weaker than that of **3**. The sensitivity of bacteria to **1** seems to be inhibited by the presence of hydroxyl groups (1, 8, 18, 20-OH) (Figures 1 and 5). An earlier study found that the high sensitivity of bacteria to **3** was promoted by four hydrogen bond interactions between four free hydroxyl groups (1, 8,

Table 2 750 MHz ^{1}H and 125 MHz ^{13}C NMR data on 1, 2 and 3

	DMSO-d_6										*CD_3OD*					
	1				***2***			***3***			***1***			***Saliniketal a***[a]		
Position	δ_C	δ_H	*Multi, J (Hz)*	*HMBC*	δ_H	*Multi, J (Hz)*	*Position*	δ_H	*Multi, J (Hz)*	*Position*	δ_C	δ_H	*Multi, J (Hz)*	δ_C	δ_H	*Multi, J (Hz)*
1	170.3									1	181.3 (br)					
2	143.1									2	143.2					
2-NH		9.14	(br s)	C-1, C-3, C-12	7.21	(br s)	15-NH	9.41	(br s)							
					7.03	(br s)										
3	111.7	7.18	(s)	C-1, C-2, C-10			3	7.29	(s)	3	116.4	7.55	(s)			
4	186.7									4	187.9					
5	117.7	6.32	(s)	C-4, C-7, C-9						5	112.7	6.96	(s)			
6	180.4 (br)[b]									6	164.5					
7	112.2									7	117.8					
8	162.1 (br)									8	172.0					
8-OH		12.55	(br s)	C-7, C-8, C-9												
9	100.6									9	106.6					
10	131.1									10	132.5					
11	7.9	1.75	(s)	C-6, C-7, C-8			13	1.61	(s)	11	8.2	2.06	(s)			
12	167.1									12	170.1			175.1		
13	127.1									13	129.7			131.4		
14	137.7	6.43	(br d, 11.3)	C-12, C-16, C-28	6.02	(br d, 11.3)	17	6.20	(dd, 10.5, 1.5)	14	138.6	6.46	(br d, 11.3)	134.1	6.17	(br d, 11.1, 1.2)
15	125.3	6.78	(dd, 15.0, 12.0)	C-17	6.57	(dd, 15.0, 11.3)	18	6.12	(dd, 15.8, 10.5)	15	127.6	6.79	(dd, 15.0, 10.9)	128.3	6.60	(dd, 15.3, 11.1)
16	145.7	6.07	(dd, 15.0, 7.5)	C-14, C-29	5.76	(dd, 15.0, 8.3)	19	5.88	(dd, 15.8, 7.5)	16	146.0	6.03	(dd, 15.0, 8.3)	142.0	5.78	(dd, 15.3, 8.4)
17	40.4	2.31	(m, 8.3, 7.5, 6.8)	C-15, C-16, C-18, C-29	2.22	(m, 7.5)	20	2.10	(m)	17	42.4	2.43	(m, 8.3, 7.5)	42.3	2.35	(m, 9.3, 8.4, 6.8)
18	73.3	3.62	(m, 7.5)		3.57	(m, 9.0)	21	3.57	(m)	18	75.8	3.78	(dd, 9.8, 1.9)	75.8	3.71	(dd, 9.3, 1.8)
18-OH		4.57	(m)		4.52	(br s)	21-OH	4.38	(m)							
19	34.3	1.71	(m)	C-20	1.73	(m)	22	1.61	(m)	19	36.4	1.83	(m, 6.8, 4.5, 1.9)	35.7	1.88	(m, 7.4, 4.9, 1.8)
20	75.6	3.33[c]	(m, 8.3, 3.8, 3.0)		3.33[c]	(m)	23	ND[d]		20	78.4	3.50	(dd, 8.3, 4.5)	78.2	3.52	(dd, 8.3, 4.9)
20-OH		4.64	(m)	C-19, C-20, C-21	4.67	(br s)	23-OH	4.38	(m)							
21	35.7	1.69	(m, 0.9)	C-31	1.69	(m, 6.8)	24	1.48	(m)	21	37.1	1.82	(br dq, 8.3, 6.8, 1.5)	37.1	1.84	(br dq, 8.3, 7.2, 1.4)
22	72.8	3.82	(br d, 10.5, 0.9)	C-20, C-21, C-31	3.83	(br d, 10.5)	25	5.01	(m)	22	75.2	3.94	(br d, 10.5, 1.5)	74.9	3.97	(br d, 10.8, 1.4)
23	33.4	1.84	(br dq, 10.5, 6.8, 3.8)		1.85	(m, 3.8)	26	1.32	(m)	23	35.3	1.97	(br dq, 10.5, 6.8, 3.8)	35.2	2.00	(br dq, 10.8, 7.3, 3.4)
24	79.1	4.14	(br dd, 6.8, 3.8)		4.15	(br dd, 6.8, 3.8)	27	ND[d]		24	81.8	4.20	(br dd, 6.8, 3.8)	81.6	4.23	(br dd, 6.3, 3.4)
25a	23.6	1.81	(m)		1.83	(m)	28	5.09	(br dd, 9.0)	25a	24.1	1.93	(m)	24.9	1.90	(m)
25b		1.77	(m)		1.76	(m)	29	6.11	(d, 12.8)	25b		1.88	(m)		1.94	(m)
26a	33.9	1.92	(m)		1.92	(m)				26a	35.4	2.02	(m)	35.1	2.05	(m)
26b		1.69	(m)		1.71	(m)				26b		1.80	(m)		1.80	(m)
27	104.2									27	106.6			106.4		
28	20.1	2.03	(br s)	C-12, C-13, C-14	1.86	(br s)	30	2.01	(br s)	28	20.7	2.07	(d, 1.1)	20.9	1.94	(d, 1.2)
29	16.2	0.90	(d, 6.8)	C-16, C-17, C-18	0.87	(d, 7.5)	31	0.84	(d, 7.5)	29	17.1	0.99	(d, 6.8)	17.1	0.96	(d, 6.8)

Table 2 Continued

	DMSO-d_6										CD_3OD					
	1				**2**			**3**			**1**			**Saliniketal a**[a]		
Position	δ_C	δ_H	*Multi, J (Hz)*	*HMBC*	δ_H	*Multi, J (Hz)*	*Position*	δ_H	*Multi, J (Hz)*	*Position*	δ_C	δ_H	*Multi, J (Hz)*	δ_C	δ_H	*Multi, J (Hz)*
30	11.1	0.91	(d, 6.8)	C-19, C-20	0.92	(d, 6.8)	32	0.86	(d, 6.8)	30	11.3	1.00	(d, 6.8)	11.1	1.02	(d, 7.3)
31	9.8	0.76	(d, 6.8)	C-20, C-21, C-22	0.75	(d, 6.8)	33	0.56	(d, 6.8)	31	10.5	0.88	(d, 6.8)	10.2	0.89	(d, 7.2)
32	12.4	0.64	(d, 6.8)	C-22, C-23, C-24	0.65	(d, 6.8)	34	0.15	(d, 6.8)	32	13.0	0.71	(d, 6.8)	12.3	0.76	(d, 7.3)
33	24.0	1.31	(s)	C-26, C-27	1.31	(s)				33	24.4	1.39	(s)	24.2	1.39	(s)
							36	1.92	(s)							
							37	2.97	(s)							
							14	1.96	(s)							

[a]Data adapted from Williams *et al*.[8]
[b]Broad peak signal.
[c]^{1}H NMR observed at 40 °C.
[d]Overrapped H_2O.

21, 23-OH) and DNA-dependent RNA polymerase.[14] Compound **2** was also found to show no significant antimicrobial activity.[8]

METHODS

Spectroscopic measurements

Optical rotations were obtained on a Horiba SEPA-300 digital polarimeter (Horiba, Kyoto, Japan). The UV spectrum pattern was measured on a Beckman DU 640 spectrometer (Beckman Coulter, Tokyo, Japan) and the IR spectrum was measured with a Jasco FT/IR-430 instrument (Jasco, Tokyo, Japan). The ^{1}H and all 2D NMR spectra (COSY (gradient-selected ^{1}H–^{1}H COSY), HSQC (gradient-selected HSQC), HMBC (gradient-selected HMBC), and ROESY) were recorded with a Varian Unity INOVA 750 instrument (Varian, Tokyo, Japan) at 750 MHz. The ^{13}C NMR spectrum was recorded on a Varian Unity INOVA 500 instrument at 125 MHz. Chemical shifts were referenced to the solvent peaks of δ_H 3.31 and δ_C 49.15 for CD_3OD and δ_H 2.49 and δ_C 39.5 for DMSO-d_6. High-resolution FAB-MS data were obtained on a Jeol JMS 700 spectrometer. LC-MS spectra were measured with a Thermo Fisher Scientific K.K. LCQ-Advantage instrument (Thermo Fisher Scientific K.K., Yokohama, Japan).

Taxonomy

The 16S rRNA gene has been identified using degenerate PCR and sequencing methods.[15] The 16S rRNA gene sequence was compared with bacterial sequence data stored in the DDBJ database by using the BLAST algorithm.[16]

Fermentation

The medium consisted of Bacto peptone (BD Difco) 5 g, yeast extract 1 g, iron (III) citrate 0.1 g, distilled water 250 ml and sea water 750 ml (pH 7.6). A 1.0 l Erlenmeyer flask containing 500 ml of medium was incubated first with a stock culture of YM23-082 and then on a rotary shaker at 30 °C for 3 days. The 5 ml samples of the seed culture were then placed in 1.0 l Erlenmeyer flasks containing 500 ml of a production medium consisting of Pharmamedia (Traders protein) 20 g, yeast extract 1 g, iron (III) citrate 0.1 g, distilled water 250 ml and sea water 750 ml (pH 7.6). Fermentation took place on a rotary shaker at 30 °C for 7 days.

LC-MS methods

All samples were analyzed by HPLC/PDA with a linear gradient from 10 to 100% CH_3CN at intervals of 1 min. The LC-MS was conducted on an Inertsil ODS-2 column (GL Sciences, Tokyo, Japan) (1.5 mm i.d. ×250 mm). The HPLC fractions were eluted at a rate of 0.1 ml min^{-1} with solvent A consisting of 0.1% formic acid/solvent B consisting of 0.1% formic acid in CH_3CN (80:20) for 5 min, followed by a linear gradient from solvent A to B for 45 min, solvent B alone for 60 min and then back to the initial solvents. The column oven temperature was set at 40 °C. The PDA (photodiode array detector) was monitored at 220–800 nm. Ionization of ESI was optimized by human angiotensin II (Sigma, Tokyo, Japan). The total ion chromatogram was alternately monitored at positive and negative ions in the mass range of *m/z* 150.0–2000.0. The capillary temperature was set at 220 °C, spray voltage was optimized to 5.2 kV and the sheath nitrogen gas flow was set at 28 arbitrary units (arb). The LC-MS spectral data were compared with those in the in-house database, NCBI database (http://pubchem.ncbi.nlm.nih.gov/) and literature values for *Salinispora* sp. metabolites.[1,6,7,17]

Extraction and isolation

The YM23-082 fermentation broth (10.0 l) was centrifuged and the mycelium extracted with MeOH, and the supernatant was then extracted with 2 times EtOAc. The combined extract was passed through filter paper (Advantec Co. Ltd., Ehime, Japan) and evaporated. Then, the extract was partitioned between EtOAc and saturated NaCl. After that, the EtOAc layer was dried with anhydrous Na_2SO_4 and evaporated. Furthermore, the EtOAc layer was partitioned between n-Hex and 90% water MeOH. The anti-A549 active 90% water MeOH layer was evaporated and chromatographed on a silica gel column with $CHCl_3$, MeOH and water. The anti-A549 eluates, $CHCl_3$/MeOH (98:2), $CHCl_3$/MeOH (97:3), $CHCl_3$/MeOH (96:4) and $CHCl_3$/MeOH (95:5), were subjected to LC-MS methods.

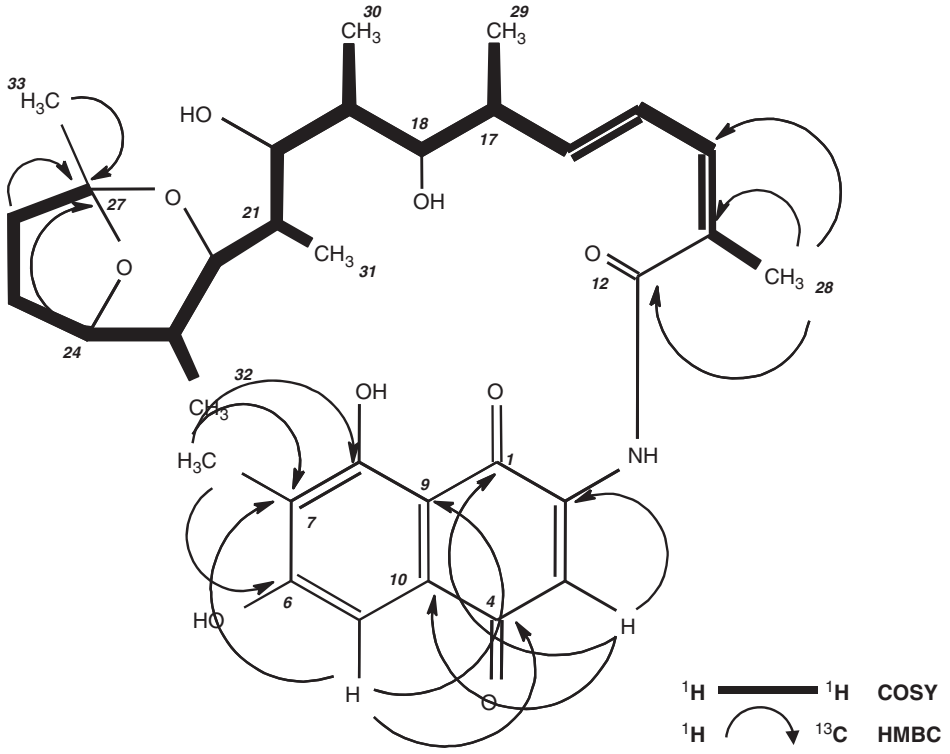

Figure 2 2D NMR spectral data in solvent CD_3OD.

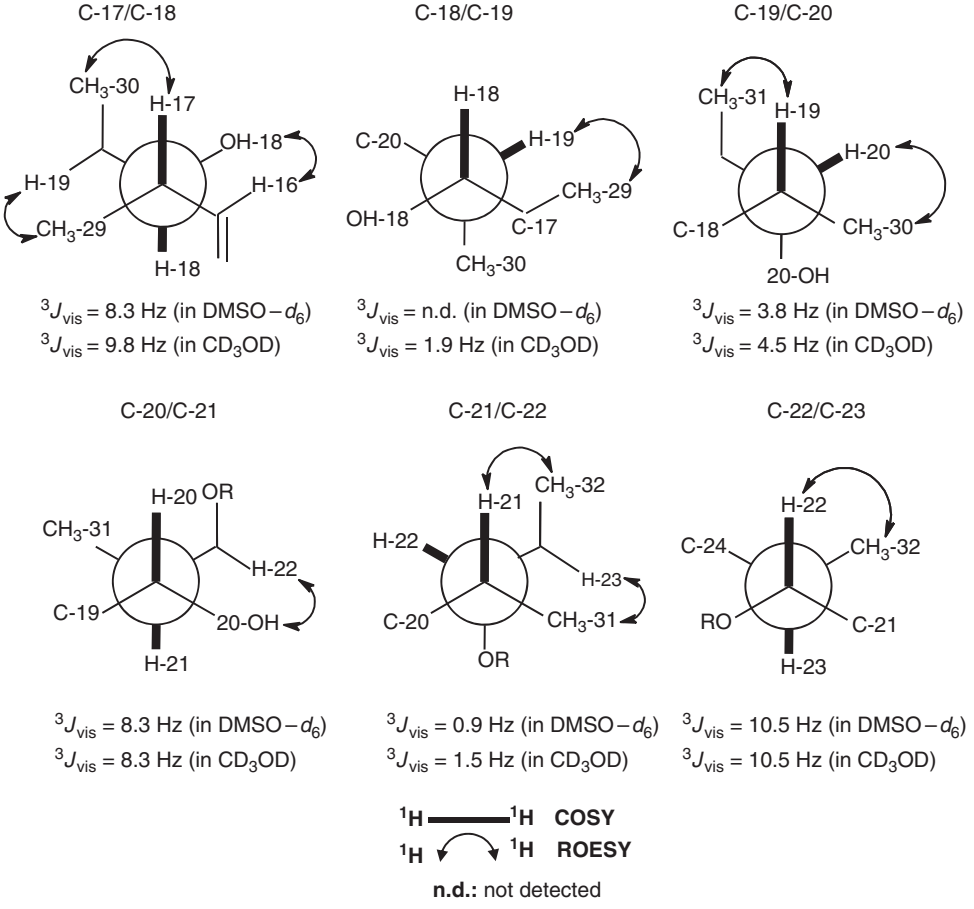

Figure 3 Data on ROESY correlations, and coupling constants and partial structures of **1**.

Salinisporamycin (1)

The UV spectrum pattern of **1** was nearly identical with the spectrum of rifamycin antibiotics.[10] However, the MW was not the same in this experiment as in the databases mentioned above. Therefore, the silica gel chromatographed eluates were separated by HPLC (Inertsil ODS-2 column, 4.6 mm i.d. ×250 mm) with a linear gradient from 10 to 100% CH_3CN to afford **1** (0.6 mg). Compound **1** LC-MS: RT, 38.4 min; PDA, 240, 270, 326, 409 nm; MS, *m/z* 598 $[M+H]^+$, *m/z* 596 $[M-H]^-$.

Saliniketal A (2)

The silica gel chromatographed eluates were separated by HPLC (Inertsil ODS-2 column, 4.6 mm i.d. ×250 mm) with isocratic elution of 30% CH_3CN to afford **2**[8,9] (2.6 mg). Compound **2** LC-MS: RT, 25.1 min; PDA, 252 nm; MS, *m/z* 396 $[M+H]^+$, n.d. $[M-H]^-$; 750 MHz, DMSO-d_6: Table 2. The chemical shifts revealed that **2** was identical with the values reported in the literature for saliniketal A.[8]

Rifamycin S (3)

The silica gel chromatographed eluates were separated by HPLC (Inertsil ODS-2 column, 4.6 mm i.d. ×250 mm) with a linear gradient from 20 to 100% CH_3CN to afford **3**[10] (4.6 mg). Compound **3** LC-MS: RT; 37.5 min, PDA; 239, 276, 334, 409 nm, MS; *m/z* 696 $[M+H]^+$, *m/z* 694 $[M-H]^-$; TLC: R_F value at 0.87 ($CHCl_3$:MeOH=4:1); UV λ_{max} nm (log ε) in MeOH: 228 (4.86), 271 (4.71), 315 (4.43), 410 (3.93); IR ν_{max} (KBr) cm^{-1}: 3431, 2926, 2854, 1710, 1606, 1465, 1415, 1384, 1354, 1259, 1164, 1074, 976; 750 MHz, DMSO-d_6:

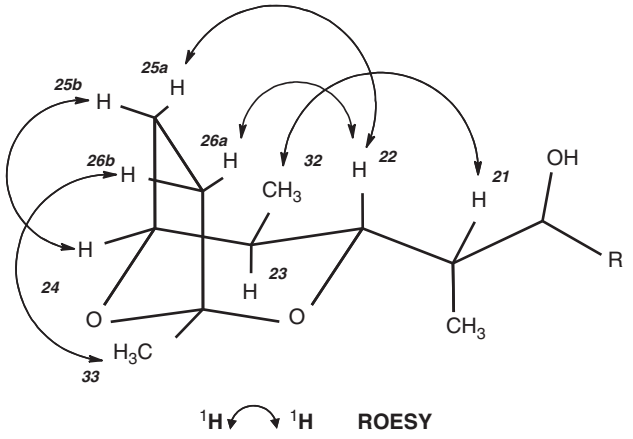

Figure 4 ROESY correlations and partial structure of **1**.

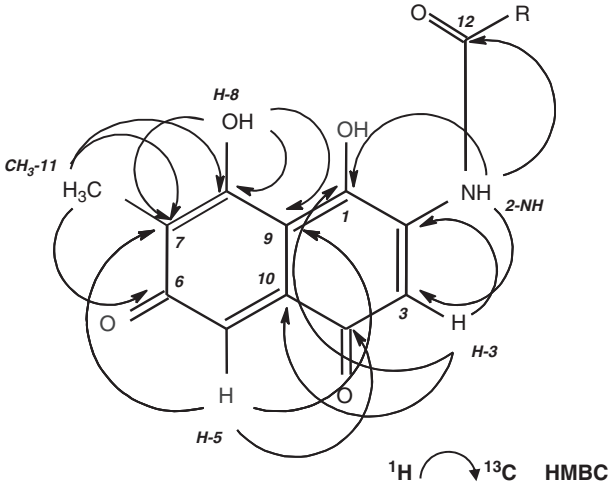

Figure 5 Heteronuclear multiple bond correlations and naphthoquinone ring system of **1** in solvent DMSO-d_6.

Table 3 750 MHz ^{1}H and 125 MHz ^{13}C NMR data of naphthoquinone ring system of 1, 31-homo rifamycin W and rifamycin Z

	CD_3OD					*DMSO-d_6*				
	1		***31-Homo rifamycin W***[a]			***1***		***Rifamycin Z***[b]		
Position	δ_C	δ_H	δ_C	δ_H	*Diff. (p.p.m.)*[c]	δ_C	δ_H	δ_C	δ_H[d]	*Diff. (p.p.m.)*
1	181.3 (br)[e]		182.3		−1.0	170.3		181.8		−11.5
1-OH		—		—			ND		—	
2	143.2		142.7		0.5	143.1		140.4		2.7
2-NH		—		—			9.14		8.90 (ND)	
3	116.4	7.55	117.6	7.52	−1.2	111.7	7.18	114.2	7.30 (7.70)	−2.5
4	187.9		187.3		0.6	186.7		184.0		2.7
5[f]	112.7	6.96	127.1	—	—	117.7	6.32	123.5	—	—
6	164.5		164.2		0.3	180.4 (br)		160.0		20.4
6-OH		—	—				—		10.50 (7.70)	
7	117.8		118.7		−0.9	112.2		117.6		−5.4
8	172.0 (br)		166.5		5.5	162.1 (br)		162.1		0.0
8-OH		—		—			12.55		12.70 (9.40)	
9	106.6		106.7		−0.1	100.6		106.5		−5.9
10	132.5		129.7		2.8	131.1		127.7		3.4
11	8.2	2.06	8.5	2.12	−0.3	7.9	1.75	8.7	2.15 (1.62)	−0.8
12	170.1		172.0		−1.9	167.1		171.6		−4.5

Abbreviation: ND, not detected.
[a]Data adapted from Wang *et al.*[12]
[b]Data adapted from Cricchio *et al.*[13]
[c]Diff. (p.p.m.)=obs. [δ_C]−ref. [δ_C].
[d]In solvent DMSO-d_6/acetone-d_6 (7:3) (Pyridine-d_5).
[e]Broad peak signal.
[f]C-6 of rifamycin Z and 31-homo rifamycin W were assigned as diagnostic of quaternary carbon signal.

Table 4 Antimicrobial activity properties of 1, 2 and 3

Taxin	*Strain*	***1***	***2***	***3***
Firmicutes	*Staphylococcus aureus* IFO 12732	0.46	37	0.0056
Firmicutes	*Bacillus subtilis* IFO 3134	4.1	111	1.4
Bacteroidetes	*Cytophaga marinoflava* IFO 14170	>200	>200	12.3
Gammaproteobacteria	*Escherichia coli* IFO 3301	>200	>200	>200
Gammaproteobacteria	*Pseudomonas aeruginosa* IF03446	>200	>200	>200
Yeast	*Candida albicans* IFO 1060	>200	>200	>200

Antimicrobial activity (MIC, $\mu g\,ml^{-1}$).

Table 2. **3** was established by 2D NMR, and the chemical shifts showed that **3** was nearly identical with the values reported in the literature for proansamycin B,[10] 8-deoxy-rifamycin[18] and 31-homorifamycin W.[12]

Cytotoxic and antibacterial activity

A549 cells were cultured in Dulbecco's modified Eagle's medium containing 10% fetal bovine serum. The cells were seeded in a flat-bottomed 96-well microplate (4000 cells per 200 µl per well), and then cultured for 14 h at 37 °C in a CO_2 incubator (5% CO_2-air). Serially diluted **1** was added to each well, and the cells were further cultured for 48 h. The number of cells was counted by Alamar Blue assay.[19] The MIC of **1**, **2** and **3** were analyzed by paper disk methods.[20]

ACKNOWLEDGEMENTS

We thank Professor Ryuichi Sakai of the Faculty Department at Kitasato University for the high-resolution FAB-MS measurements. We are also grateful for the technical assistance of Ms Kumiko Kawahata, Ms Thie Ohshima and Ms Tomoe Sasaki. This work was performed as part of the project entitled 'Construction of a Genetic Resource Library of Unidentified Microorganisms' supported by the New Energy and Industrial Technology Development Organization (NEDO).

1 Bull, A. T. & Stach, J. E. M. Marine actinobacteria: new opportunities for natural product search and discovery. *Trends Microbiol.* **15,** 491–499 (2007).
2 Blunt, J. W. *et al.* Marine natural products. *Nat. Prod. Rep.* **25,** 35–94 (2008).
3 Smyth, W. F. & Rodriguez, V. Recent studies of the electrospray ionization behaviour of selected drugs and their application in capillary electrophoresis–mass spectrometry and liquid chromatography-mass spectrometry. *J. Chromatogr. A* **1159,** 159–174 (2007).
4 Corcia, A. D. & Nazzari, M. Liquid chromatographic–mass spectrometric methods for analyzing antibiotic and antibacterial agents in animal food products. *J. Chromatogr. A* **974,** 53–89 (2002).
5 Maldonado, L. A. *et al. Salinispora arenicola* gen. nov., sp. nov. and *Salinispora tropica* sp. nov., obligate marine actinomycetes belonging to the family *Micromonosporaceae*. *Int. J. Syst. Evol. Microbiol.* **55,** 1759–1766 (2005).
6 Jensen, P. R., Williams, P. G., Oh, D. C., Zeigler, L. & Fenical, W. Species-specific secondary metabolite production in marine actinomycetes of the genus *Salinisporara*. *Appl. Environ. Microbiol.* **73,** 1146–1152 (2007).
7 Udwary, D. W. *et al.* Genome sequencing reveals complex secondary metabolome in the marine actinomycete *Salinispora tropica*. *Proc. Natl Acad. Sci. USA* **104,** 10376–10381 (2007).
8 Williams, P. G. *et al.* Saliniketals A and B, Bicyclic Polyketides from the Marine Actinomycete *Salinispora arenicola*. *J. Nat. Prod.* **70,** 83–88 (2007).
9 Paterson, I., Razzak, M. & Anderson, E. A. Total synthesis of (–)-Saliniketals A and B. *Org. Lett.* **10,** 3295–3298 (2008).
10 Stratmann, A. *et al.* New insights into Rifamycin B biosynthesis: isolation of Proansamycin B and 34a-Deoxy-rifamycin W as early macrocyclic intermediates indicating two separated biosynthetic pathways. *J. Antibiot.* **55,** 396–406 (2002).
11 Hoch, J. C., Dobson, C. M. & Karplus, M. Vicinal coupling constants and protein dynamics. *Biochemistry* **24,** 3831–3841 (1985).
12 Wang, N. J., Han, B. L., Yamashita, N. & Sato, M. 31-homorifamycin W, a novel metabolite from *Amycolatopsis mediterranei*. *J. Antibiot.* **47,** 613–615 (1994).
13 Cricchio, R. *et al.* Rifamycin Z, a novel ansamycin from a mutant of *Nocardia Mediterranea*. *J. Antibiot.* **34,** 1257–1260 (1981).
14 Floss, H. G. & Yu, T. W. Rifamycin–mode of action, resistance, and biosynthesis. *Chem. Rev.* **105,** 621–632 (2005).
15 Hayakawa, Y. *et al.* Piericidins C_7 and C_8, new cytotoxic antibiotics produced by a marine *Streptomyces* sp. *J. Antibiot.* **60,** 196–200 (2007).
16 Altsuchul, S. F., Gish, W., Miller, W., Myers, E. W. & Lipman, D. J. Basic local alignment search tool. *J. Mol. Biol.* **215,** 403–410 (1990).
17 Hewavitharana, A. K., Shaw, P. N., Kim, T. K. & Fuerst, J. A. Screening of rifamycin producing marine sponge bacteria by LC–MS–MS. *J. Chromatogr. B* **852,** 362–366 (2007).
18 Ghisalaba, O, Traxer, P, Fuhrer, H & Richer, W. J Early intermediates in the biosynthesis of Ansamycins III and identification of further 8-deoxyansamycins of the rifamycin type. *J. Antibot.* **33,** 847–856 (1980).
19 Matsuo, Y. *et al.* Urukthapelstatin A, a novel cytotoxic substance from marine--derived *Mechercharimyces asporophorigenens* YM11-542 I. fermentation, isolation and biological activities. *J. Antibiot.* **60,** 251–255 (2007).
20 Jang, J. H., Kanoh, K., Adachi, K. & Shizuri, Y. New dihydrobenzofuran derivative, Awajanoran, from marine-derived *Acremonium* sp. AWA16-1. *J. Antibiot.* **59,** 428–431 (2006).